The following publication X. Lyu, J. Zhao, Y. Jia, Z. Xu and K. Po Wong, "Coordinated Control Strategies of PMSG-Based Wind Turbine for Smoothing Power Fluctuations," in IEEE Transactions on Power Systems, vol. 34, no. 1, pp. 391-401, Jan. 2019 is available at https://doi.org/10.1109/TPWRS.2018.2866629.

Coordinated Control Strategies of PMSG-based Wind Turbine for Smoothing Power Fluctuations

Xue Lyu, *Student Member, IEEE*, Jian Zhao, *Student Member, IEEE*, Youwei Jia, *Member, IEEE*, Zhao Xu, *Senior Member, IEEE*, Kit Po Wong, *Fellow, IEEE*

***Abstract*—High penetration of wind energy in the modern power system exposes the need of smoothing the fluctuating output power in an effective and conducive way. In this context, this paper proposes two novel control strategies that utilize the self-capability of permanent magnet synchronous generator based wind turbine to realize power smoothing. The first strategy pursues to offer power smoothing support via simultaneous utilization of DC-link voltage control, rotor speed control and pitch angle control. The second control strategy seeks to coordinate the three concerned individual control schemes in a hierarchical manner, where the power smoothing tasks are allocated to individual control modules or their combinations dynamically in line with WT's operation status. Both two strategies are able to provide power smoothing support by fully exploiting wind turbine's self-capability, whereas the second strategy has the merits on 1) reducing the activation frequency of pitch angle control, and 2) enhancing wind energy harvesting. Case studies of the proposed control strategies are carried out to compare and verify their effectiveness in achieving power smoothing.**

***Index Terms*-- Permanent magnet synchronous generator(PMSG), power smoothing, simultaneous control, hierarchical control.**

I. Introduction

IN the last decades, wind energy has exhibited a dramatic increase due to energy crisis and environmental issues. Though wind energy is a clean and efficient resource, high penetration of wind power can lead to detriment of power quality due to its uncertain and intermittent nature[1-3]. In industry, the variable speed wind turbines (VSWTs) are widely utilized due to their high efficiency and low cost. However, the nonsynchronous grid connection of VSWTs and their free-running operation mode intensifies output power fluctuations and thereby threaten the power system security. In particular, fast fluctuation of wind power output can result in frequency variation, system instability [4-6], variation of reactive power loss and voltage flicker at the point of common coupling (PCC) to the main grid [7]. In addition, wind power fluctuations lead to other technical and economic issues. For example, wind power fluctuations result in less operational efficiency of thermal units as discussed in[8]. Generally, power reserve would be increased to counterbalance wind power fluctuations, which consequently result in higher reservation cost[9]. Furthermore, high wind penetration may require high transmission capacity, which in turn increases the transmission losses[10]. It is straightforward that wind power fluctuations bring about more operational challenges especially in the islanded power systems, of which the inertia is low and the system is weak. In this context, smoothing power fluctuations can be quite beneficial to the islanded power systems.

In order to ensure system operation security and reliability, smoothing the wind power fluctuation is desirable especially for islanded systems which have limited power reverse. The fluctuated power can seemingly be alleviated owing to the intrinsic temporal and spatial coupling in one or more wind farms. However, such aggregation effect is naturally flawed with limited smoothing capability considering volatile wind direction and fixed location of wind turbine (WT) installation [11]. In this sense, it is still worthy of further investigation of advanced control to exploit individual WTs full potential of power smoothing. Thus far, this research direction has attracted wide attention in both industry and academia over the last decade, which can be categorized into two classes. The first class is to utilize energy storage system (ESS) to store the excessive energy and release back once needed. In [12], an ultra-capacitor (UC) bank and a lithium-ion battery bank (LB) are utilized to mitigate the short-term and long-term wind power fluctuation, respectively. Other ESSs such as flywheel and upper conducting magnetic energy storage (SMES) have also been considered in [13-17]. Nevertheless, such approaches inevitably involve additional investments. Distinguished from the previous approaches that rely on additional ESS, the second class is aimed to delve into the greatest potential of the WT itself for power smoothing. This type of strategies is advantageous over ESSs based ones owing to less investment cost and maximum utilization of the existing resources of WT. Such resources comprising of the following three aspects can be synthesized as the self-capability of WTs for power smoothing.

The first resource lies in the energy harvesting capability through pitch angle adjusting. An effective pitch angle control can directly affect the active power output of WTs. To achieve such control objective, fuzzy logic pitch controllers are reported in [18, 19] to smooth wind power fluctuations under below-rated wind speed conditions. Those controllers are reported to be robust and easy to be implemented. However, it

This work was supported by Hong Kong RGC Theme Based Research Scheme Grants No. T23-407/13N and T23-701/14N.

X. Lyu, J. Zhao, Y. Jia and Z. Xu are with the Department of Electrical Engineering, The Hong Kong Polytechnic University, Hung Hom, Hong Kong. (emails:16900948r@connect.polyu.hk,zhaojianzju@gmail.com,jiayouwei@gmail.com,eezhaoxu@polyu.edu.hk).

K. P. Wong is with Department of Electrical and Electronic Engineering, The University of Western Australia, Perth, Australia. (email: kitpo@ieee.org)

is noted that the wind energy harvesting efficiency is low since the curtailed wind power is directly discarded. In addition, frequent activation of pitch angle adjustment will inevitably increase mechanical stress and fatigue of WTs.

Another resource that can be utilized to smooth out wind power fluctuation is the kinetic energy (KE) stored in the rotational rotor [20-22]. When the smoothing command is received, the rotating mass releases or absorbs excessive energy via rotor speed deceleration/acceleration. To establish the relationship between smoothing command and rotor speed, a fuzzy PID controller is proposed in [22] to replace the conventional speed controller. In [21], the frequency deviation is introduced to the controller by utilizing KE. Even though the operating point of WT is shifted away from maximum power point (MPP) when rotor speed control is adopted, it has an advantage as compared to pitch angle control in energy harvesting since a portion of the curtailed energy can be stored in the rotational rotor as KE.

The last source can be exploited is the DC-link capacitor of WT. It is observed that DC-link voltage can be temporarily changed so as to release or absorb a part of energy. Based on such control mechanism, A DC-link voltage control strategy is proposed in [23, 24] to smooth out the high-frequency domain power fluctuations, where the DC-link voltage reference is determined by the ratio of output power fluctuations and DC-link current. However, the performance of the control method proposed in [23, 24] is significantly influenced when DC-link voltage reaches its limits, at which DC-link current shall become zero and thereby the voltage reference would go to infinity. In comparing pitch angle and rotor speed controls, taking advantage of capacitor energy becomes the most preferable option as the introduced DC-link voltage control never affect the maximum power point tracking (MPPT) control. However, it is admitted that the usable energy is relatively small.

The second class of the smoothing strategies is very promising whereas current research in this particular area is still at its infant stage. It is challenging to coordinate and implement the control strategies of DC-link voltage, rotor speed and pitch angle in an effective way. In the existing literature, how to manage those concerned controls for power smoothing has not been well analyzed. To fill in this gap, this paper extensively investigates all existing control resources of WTs and efficiently coordinate them to accommodate various system operating conditions.

Motivated by the aforementioned analysis, this paper proposes two power smoothing control schemes for PMSG-based WT through the newly proposed DC-link voltage control, rotor speed control and pitch angle control. The first scheme pursues to smooth the power by simultaneously utilizing these three control strategies. This control method requires frequent activation of rotor speed control and pitch angle control in response to power fluctuations. This simply forces the operating point of WT constantly deviating from maximum power point (MPP). It is straightforward that such controller may suffer from a semi-optimal effect in considering WT mechanical fatigue, energy harvesting rate and so forth. To overcome this drawback, the second strategy aims to utilize these three resources in a hierarchical manner. Specifically, the smoothing task is intelligently fed into each individual controller based on a newly proposed rule-based algorithm. Both the two proposed control schemes are verified through extensive case studies. The performance exhibits that power fluctuations can be effectively managed and reduced.

II. Modeling of PMSG-based Wind Turbine

The system configuration of PMSG-based WT is depicted in Fig. 1. The WT is directly connected with the permanent magnet synchronous generator (PMSG), which is further connected to the main grid through a full-capacity back-to-back converter. The operation principle of the back-to-back converter is to synchronize the current with variable amplitude along with the frequency of the grid. MPPT control is achieved by the generator side converter and the DC-link voltage is regulated by the grid side inverter [25].

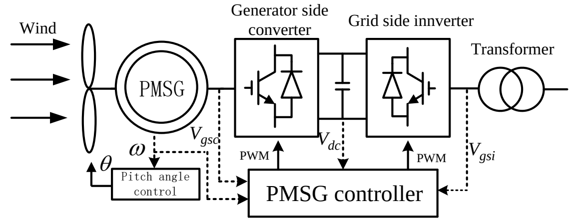

Fig. 1. System configuration of a PMSG-based wind turbine

The mechanical power extracted from the wind is defined as,

$$P_{wt} = \frac{\rho}{2}\pi R^2 v_w{}^3 C_p(\lambda,\beta) \tag{1}$$

where ρ is the air density, R is the rotor blade radius, v_w is the wind speed, λ is the tip speed ratio, β is the pitch angle, and C_p is the power coefficient. The power coefficient is a nonlinear function between tip speed ratio and pitch angle. As reported in [26], it can be formulated as,

$$C_p = 0.22(\frac{116}{\lambda_i} - 0.4\beta - 5)e^{-\frac{12.5}{\lambda_i}} \tag{2}$$

$$\frac{1}{\lambda_i} = \frac{1}{\lambda + 0.08\beta} - \frac{0.035}{\beta^3 + 1} \tag{3}$$

where the tip speed ratio is represented as,

$$\lambda = \frac{\omega R}{v_w} \tag{4}$$

where ω is the rotor speed. Fig. 2 shows the relationship between the power coefficient C_P and tip speed ratio. Upon certain wind speed, pitch angle control (i.e. $\beta \neq 0$) can lead to considerable power curtailment, which is reflected as down shift of curve in Fig. 2. As expressed in Eq (4), there exists a unique WT rotor speed that corresponds to the maximum power coefficient.

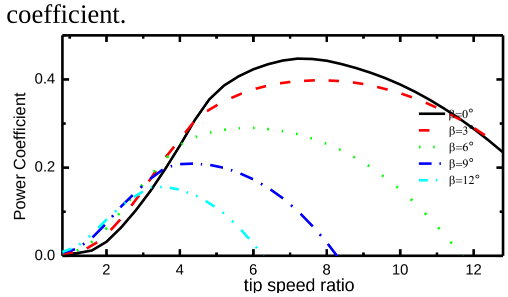

Fig. 2 The $C_p - \lambda$ characteristics

To avoid excessive rotor acceleration under high-speed wind conditions, pitch angle control is activated to limit the captured wind energy and keep the rotor speed at the reference value ω_{max}. Fig. 3 shows the conventional pitch angle control scheme. The error signal between ω_{max} and the measured rotor speed ω_{meas} are sent to a PI controller, which produces the pitch angle reference. The limitation of the pitch angle is within 0°-90°, and the maximum changing rate of pitch angle is within [-5°/s, 5°/s].

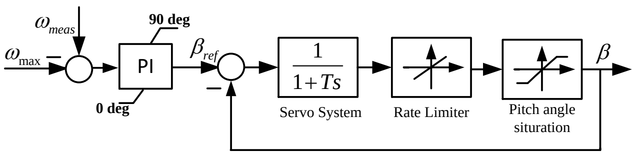

Fig. 3. Conventional pitch angle control

III. Simultaneous Control Strategy for Wind Power Smoothing

In this approach, a smoothing command is generated via the exponential moving average (EMA) algorithm. Meanwhile, novel control schemes regarding DC-link voltage, rotor speed and pitch angle are individually proposed. In introducing the smoothing command towards each individual controller, they are able to respond simultaneously to provide power smoothing support.

A. Proposed Power Smoothing Command

In order to implement the smoothing control strategy, a preferable power smoothing reference should be predefined for WT to follow. There are many methods to obtain such a smoothing command. A low pass filter introduced in [20, 23, 27]aims to generate a preferable power smoothing command, of which the output is greatly dependent on the selected filter time constant. A simple moving average method is employed to produce a smoothing command in [28], and the smoothing effect is dependent on the length of the selected time window. System frequency can also be introduced to adjust the active power [21, 29], in which the required output adjustment is determined by the gain of the frequency deviation loop. In this paper, the EMA algorithm is adopted considering its advantage of the ease of calculation and implementation, though more advanced smoothing algorithm deserves further investigations. The smoothing command can be generated as,

$$P_{com}(t) = [(P_{current} - P_{com}(t-1)) \times k] + P_{com}(t-1) \tag{5}$$

where P_{com} is the smoothing command calculated by EMA, $P_{current}$ is the real-time measured wind power output. k is the weighting factor. For the period-based EMA, the weighting factor k can be calculated as k=2/(N+1), where N is a specified number of periods. For practical application, N can be specified by the system operators. In general, the larger the N value is, the smoother the obtained command will be.

B. DC-link Voltage Control

The voltage of DC-link capacitor reflects the power balance between the power injected into the generator side converter and the power transmitted to the grid side inverter. In

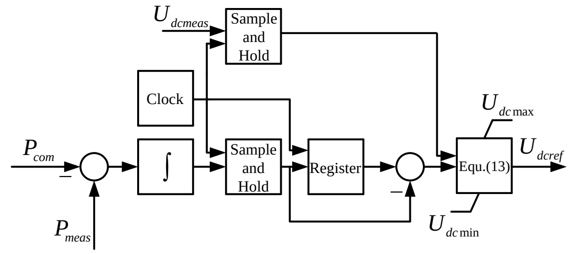

Fig. 4. Control scheme of the proposed DC-link voltage control

conventional control scheme, the DC-link voltage reference is set as a constant (i.e. 1 p.u.) and the capacitor does not provide power smoothing ability. The dynamics of DC-link voltage can be written as follows in per unit form,

$$C_{dc}U_{dc}\frac{dU_{dc}}{dt} = P_{gsc} - P_{gsi} \tag{6}$$

$$C_{dc} = CU_{dcB}^2 / S_B \tag{7}$$

where P_{gsc} is the power injected into the generator side converter, P_{gsi} is the power transmitted to the grid side inverter, C_{dc} is the capacitance in p.u., U_{dc} is the DC-link voltage in p.u., C is the capacitance of DC-link capacitor, U_{dcB} is the base value of DC-link voltage, and S_B is the base value of nominal capacity of WT.

In practice, the DC-link voltage varies within a small range in the normal operation. According to [30], the controllable region of DC-link voltage is dependent on the insulation requirements, current ratings and PWM functionality. In our work, the DC-link voltage deviation constraints are set between ±0.14p.u. to avoid excess voltage volatility. It should be noted that such settings can be tuned flexibly by the intrinsic characteristic of power electronic devices. To this end, DC-link capacitor can release/absorb extra energy during its discharging/charging period by following the smoothing command P_{com}. In this process, the power delivered to grid P_{gsi} can be replaced by the generated smoothing command. As a result, a modified dynamic equation of DC-link voltage can be rewritten as,

$$C_{dc}U_{dc}\frac{dU_{dc}}{dt} = P_{gsc} - P_{com} \tag{8}$$

The stored/released energy can be represented by integrating Eq(8) over time,

$$\int_{t_0}^{t_1} C_{dc}U_{dc}dU_{dc} = \int_{t_0}^{t_1}(P_{gsc} - P_{com})dt \tag{9}$$

$$\frac{1}{2}C_{dc}(U_{dc1}{}^2 \text{-} U_{dc0}{}^2) = \int_{t_0}^{t_1}(P_{gsc} - P_{com})dt \tag{10}$$

where U_{dc0} and U_{dc1} denote the DC-link voltage of the previous and current moment, respectively. As U_{dc1} can be expressed in terms of voltage deviation ΔU_{dc} , substituting $U_{dc1} = U_{dc0} + \Delta U_{dc}$ into Eq (10), one can obtain,

$$\frac{1}{2}C_{dc}[(U_{dc0} + \Delta U_{dc})^2 - U_{dc0}{}^2] = \int_{t_0}^{t_1}(P_{gsc} - P_{com})dt \tag{11}$$

$$\frac{1}{2}C_{dc}[2U_{dc0}\Delta U_{dc} + \Delta U_{dc}{}^2] = \int_{t_0}^{t_1}(P_{gsc} - P_{com})dt \tag{12}$$

In considering ΔU_{dc} is set within ±0.14 p.u. in this paper, the quadratic term of voltage deviation ΔU_{dc}^2 can be neglected.

Derived from Eq (12), the required DC-link voltage reference U_{dc1} can be calculated according to,

$$U_{dc1} = U_{dc0} + \frac{\int_{t_0}^{t_1} (P_{gsc} - P_{com})dt}{C_{dc} U_{dc0}} \tag{13}$$

Finally, a novel DC-link voltage control scheme is designed and introduced to the grid side inverter, as shown in Fig. 4, where P_{meas} is the measured actual power output of WT, U_{dcref} is the generated reference value of the DC-link voltage. The control mechanism is to establish the relationship between the smoothing command and the new DC-link voltage reference. A sample and hold routine is introduced to store the measured DC-link voltage at the previous moment so that continuous calculation of the subsequent reference values can be served. The register model is a digital shifting register. With every rising edge of the clock signal, the values are shifted by one, then the input is read and stored. As a result, the released/absorbed energy from time t_0 to t_1 is obtained based on the sample and hold routine and a register routine. And then, the required DC-link voltage is calculated based on Eq (13) and is tracked as the new reference for the outer loop voltage and inner loop current controls of the grid-side inverter.

C. Rotor Speed Control

The rotor speed dynamics is governed by the rotor motion equation described as follows,

$$2H\omega \frac{d\omega}{dt} = P_{wt} - P_{mpp} \tag{14}$$

where P_{mpp} denotes the reference active power from the MPPT algorithm, H denotes the inertia constant, which can be defined as,

$$H = \frac{J \omega_{nom}^{2}}{2P_N} \tag{15}$$

where ω_{nom} is the nominal rotational speed, J is the inertia, which can be calculated by,

$$J = J_{tur} + J_{gen} \tag{16}$$

where J_{tur} is the turbine inertia and J_{gen} is the generator inertia.

The core idea of rotor speed control is to utilize the energy stored in the rotating rotor to smooth output power. The active power reference of a PMSG can be adjusted to a new value quickly. When the smoothing command is introduced, the P_{mpp} in Eq(14) is replaced by P_{com}, hence a modified rotor motion equation can be obtained,

$$2H\omega \frac{d\omega}{dt} = P_{wt} - P_{com} \tag{17}$$

By integrating (17) over time from t_0 to t_1, one can obtain,

$$2\int_{t_0}^{t_1} H\omega d\omega = \int_{t_0}^{t_1} (P_{wt} - P_{com})dt \tag{18}$$

$$H(\omega_1^2 - \omega_0^2) = \int_{t_0}^{t_1} (P_{wt} - P_{com})dt \tag{19}$$

where ω_0 and ω_1 denote the rotor speed of the previous and current moments, respectively. ω_1 can be expressed in terms of rotor speed deviation $\Delta\omega$, defined as $\omega_1 = \omega_0 + \Delta\omega$. Substituting the above equation into Eq (19), it becomes,

$$H[(\omega_0 + \Delta\omega)^2 - \omega_0^2] = \int_{t_0}^{t_1} (P_{wt} - P_{com})dt \tag{20}$$

$$H[2\omega_0 \Delta\omega + \Delta\omega^2] = \int_{t_0}^{t_1} (P_{wt} - P_{com})dt \tag{21}$$

For a short period of time, $\Delta\omega^2$ is vanishing. Based on Eq (21), ω_1 can be calculated as:

$$\omega_1 = \omega_0 + \frac{\int_{t_0}^{t_1} (P_{wt} - P_{com})dt}{2H\omega_0} \tag{22}$$

Lastly, a new rotor speed control scheme is devised and deployed to the generator side inverter, as shown in Fig. 5. The core idea is to calculate the new rotor speed reference according to Eq (22) with the purpose of providing smoothing support. Similar with DC-link voltage control, a sample and hold routine is introduced to store the measured rotor speed at the previous moment. To avoid excessive acceleration or deceleration, the upper limit ω_{max} is predefined as 1.22p.u. and the lower limit ω_{min} is predefined as 0.7p.u. The torque reference value is obtained based on the calculated rotor speed reference value and the smoothing command. As a result, the new active power reference is obtained to smooth out power fluctuations through available KE and avoid excessive deceleration of rotor speed in the meantime. Likewise, the calculated active power is tracked as the reference of the outer loop power and inner loop current controls of the generator-side converter.

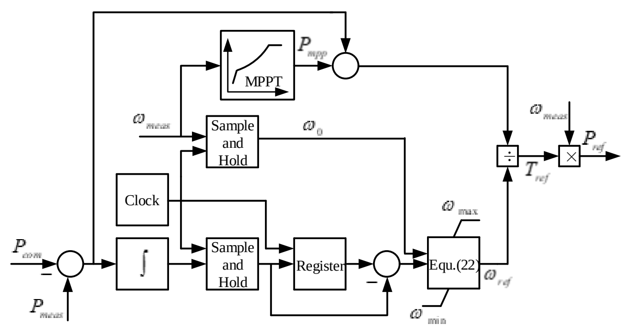

Fig. 5. Control scheme of the proposed rotor speed control

D. Pitch Angle Control

To reduce power fluctuation when wind speed rises dramatically, the smoothing command is introduced to the conventional pitch angle control to guide and determine a new pitch angle reference. The control scheme is illustrated in Fig. 6. It can be seen that the deviation between the captured wind power P_w and P_{com} are sent to a PI controller and the reference pitch angle is generated through the conventional pitch angle control framework.

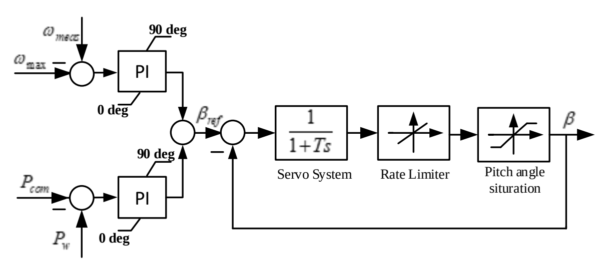

Fig. 6. Control scheme of proposed pitch angle control

E. Further Discussion of Simultaneous Control

In the simultaneous control, the identical control reference (i.e. smoothing command) is fed into all individual controllers concurrently. The active power support provided by WT comprises of three parts can be expressed as,

$$P_{\text{support}} = P_{dc} + P_{rotor} + P_{pitch} = CU_{dc}\frac{dU_{dc}}{dt} + 2H\omega\frac{d\omega}{dt} + \frac{\rho\pi R^2}{2}\left(C_p^{'} - C_p\right)v_w^3 \quad (23)$$

where $C_p^{'}$ is the new power coefficient when pitch angle control is activated.

The simultaneous control pursues to provide smoothing support via simultaneous utilization of DC-link capacitor energy, KE, and power adjusting ability of pitch angle, which makes full use of the existing resources of WT to support power smoothing. It is obvious that the proposed simultaneous control has greater smoothing capability than individual control does.

IV. Hierarchical Control Strategy for Wind Power Smoothing

Though the simultaneous control is simple to implement, it is not a cost-efficient strategy since no coordination exists among these three individual controls. This leads to less utilization efficiency of the DC-link capacitor and rotational rotor on energy storage. In addition, a certain amount of energy loss can never be avoided due to frequent activation of pitch control.

To resolve the aforementioned problem, a hierarchical control strategy is proposed to further exploit WT power smoothing potential. This strategy aims at integrating the advantages of the traditional simultaneous control and cascading control in the following aspects: 1) The three individual control schemes are adopted as per a predefined list. Such list implies the utilization priority of the smoothing resources; 2) The smoothing ability of each resource is real-time evaluated so that all controllers can individually or collectively operate in an effective way governed by an intelligent rule-based algorithm. Toward this end, the smoothing potential of the WT can be fully utilized.

The proposed hierarchical control consists of three steps. Firstly, an activation priority is designed to be i) DC-link voltage control, ii) rotor speed control, and iii) pitch angle control. Secondly, the power smoothing abilities of these control strategies are real-time evaluated. Thirdly, an intelligent rule-based task allocation strategy is proposed to optimally assign the smoothing task to each controller. In the first step, the smoothing priority is determined by the existing resources.

A. Smoothing Task Allocated to DC-link Voltage Control

The smoothing effect of DC-link voltage control is greatly dependent on the released/stored energy of the DC-link capacitor. And then the smoothing capability of DC-link capacitor is defined in the following.

Definition 1: Taking the amount of the available energy in the DC-link capacitor into consideration, the smoothing capability of DC-link capacitor at time instance *t* is proportional to the square of DC-link voltage, which is expressed as:

$$\Delta P_C(t) = \begin{cases} \Delta P_C^{\max}\dfrac{U_{dc}^2(t) - U_{dc\max}^2}{U_{dc\max}^2 - U_{dc\min}^2}, \Delta P < 0 \\ \Delta P_C^{\max}\dfrac{U_{dc}^2(t) - U_{dc\min}^2}{U_{dc\max}^2 - U_{dc\min}^2}, \Delta P > 0 \end{cases} \quad (24)$$

where $\Delta P_C^{\max}$ is the maximum active power that can be provided by DC-link capacitor, which can be determined by the capacitance, $U_{dc}(t)$ is the DC-link voltage at time instance *t*, ΔP is the deviation between the smoothing command and actual power output.

Since $\Delta P_C(t)$ should be continuously updated, the control variable $\Delta P_1(t)$ fed into DC-link voltage controller is given as follows,

$$\Delta P_1(t) = \begin{cases} \Delta P, & |\Delta P| \le |\Delta P_c(t)| \\ \Delta P_c(t), & |\Delta P| > |\Delta P_c(t)| \end{cases} \quad (25)$$

Eq (25) indicates that when the power deviation ΔP is within the smoothing ability of DC-link capacitor, the smoothing task $\Delta P_1(t)$ is directly set as ΔP , Otherwise, $\Delta P_1(t)$ is set as its maximum smoothing capability at the time instance *t*.

B. Smoothing Task Allocated to Rotor Speed Control

Similar to DC-link voltage control, the smoothing ability of rotor speed control counts on the available energy that can be released/stored by the rotational rotor. The smoothing capability of rotational rotor is defined in the following.

Definition 2: Taking the amount of the available kinetic energy in the rotational rotor into consideration, the smoothing capability of rotational rotor at time instance *t* is proportional to the square of rotor speed, which is expressed as:

$$\Delta P_R(t) = \begin{cases} \Delta P_R^{\max}\dfrac{\omega^2(t) - \omega_{\max}^2}{\omega_{\max}^2 - \omega_{\min}^2}, \Delta P < 0 \\ \Delta P_R^{\max}\dfrac{\omega^2(t) - \omega_{\text{opt}}^2}{\omega_{\max}^2 - \omega_{\min}^2}, \Delta P > 0 \end{cases} \quad (26)$$

where $\Delta P_R^{\max}$ is the maximum active power that can be released/absorbed by rotational rotor, which can be determined by the rotor inertia, $\omega(t)$ is the rotor speed at time instance t, ω_{opt} is the rotor speed at MPP status. The reason that we set ω_{opt} is to avoid excessive rotor speed deceleration, which may cause WT trip off.

Given that $\Delta P_R(t)$ should be continuously updated, the control variable $\Delta P_2(t)$ fed into rotor speed controller is calculated as follows,

$$\Delta P_2(t) = \begin{cases} 0, |\Delta P| \le |\Delta P_C(t)| \\ \Delta P - \Delta P_C(t), |\Delta P_C(t)| < |\Delta P| \le |\Delta P_C(t)| + |\Delta P_R(t)| \\ \Delta P_R(t), |\Delta P| > |\Delta P_C(t)| + |\Delta P_R(t)| \end{cases} \quad (27)$$

Eq (27) indicates that the rotor speed control will be activated only if ΔP exceeds the smoothing ability of DC-link voltage control. And when the surplus power deviation is within the smoothing ability of rotational rotor, the surplus power deviation is directly allocated to rotor speed control module. Otherwise, $\Delta P_2(t)$ is set as its maximum smoothing capability at the time instance t.

C. Smoothing Task Allocated to Pitch Angle Control

To compliment the deficit smoothing support, pitch angle control shall be activated, which however is at the lowest priority. The smoothing task allocated to pitch angle control is expressed as,

$$\Delta P_3(t)=\begin{cases}0, \Delta P\le|\Delta P_C(t)|+|\Delta P_R(t)|\\ \Delta P-|\Delta P_C(t)|-|\Delta P_R(t)|, \Delta P>|\Delta P_C(t)|+|\Delta P_R(t)|\end{cases} \tag{28}$$

As the strategy being governed by Eq (28), it is ensured that pitch angle control will not be activated when DC-link capacitor and rotational rotor are capable of storing the excessive power. On the contrary, the surplus power deviation will be managed by pitch angle control.

Fig. 7 illustrates the proposed rule-based algorithm mentioned above for hierarchical smoothing control.

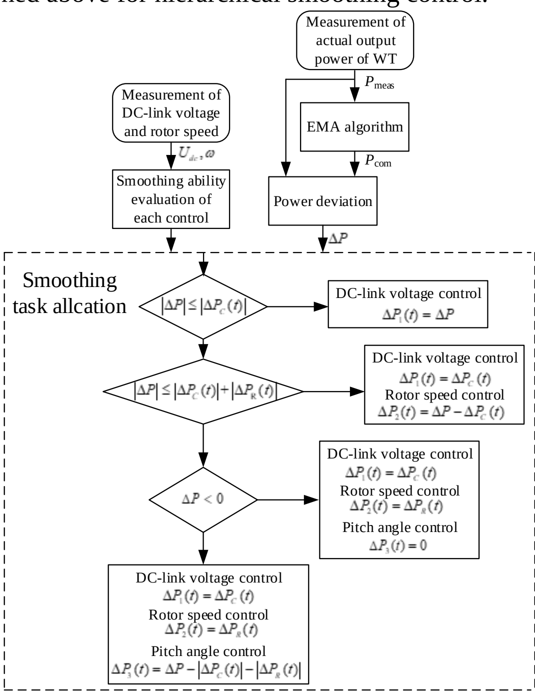

Fig. 7. Flowchart of the proposed hierarchical control

D. Further Discussion of Hierarchical Control

Admittedly, all the existing resources in the WT system that can be used to smoothen power output include DC-link capacitor, kinetic energy in the rotational system and power curtailment capability through pitching control. In the proposed hierarchical control and simultaneous control, all the existing resources are utilized to trace the power command. Theoretically, it can be well justified that the proposed smoothing-task-allocation priority is superior as compared to individual controls and simultaneous control. In the proposed hierarchical control strategy, firstly, DC-link capacitor should preferably be utilized owing to its fast-responding capability for charging/discharging certain yet limited amount of energy. Secondly, to complement the limitation of DC-link capacitor, rotational system can store/release more in form of kinetic energy. Thirdly, pitch angle control is lastly activated if significant power curtailment is needed. In this sense, well coordination of these three resources by following this control priority is able to smooth wind power output with high energy utilization efficiency. On the other hand, additional benefits can be obtained including 1) DC-link capacitor over charging/discharging can be well avoided (refer to Eq(24)); 2) excessive acceleration/deceleration of rotor speed can be avoided, which is bounded within [ω_{opt} , ω_{max}] (refer to Eq(26)); 3) actuation time of pitch angle control would be reduced so as to mitigate operational wear; and 4) excessive energy can be readily stored in DC-link capacitor and WT rotational system to reduce wind energy harvesting loss. Based on the discussion above, the proposed hierarchical strategy can achieve better energy utilization efficiency in smoothing wind power as compared to the simultaneous control strategy.

The proposed hierarchical control can also be applicable to the wind farm. On the level of wind farm (without considering wake effect), the smoothing task is delivered to each control module of WT based on the predefined priority and the smoothing capability calculation module. In this sense, all WTs operate in a distributed way to enhance total wind energy harvesting and reduce the activation frequency of pitch angle control in satisfying the smoothing command.

V. CASE STUDIES

A. Simulation Model and Parameter Setup

To verify the effectiveness of the proposed control strategies, a test system (as shown in Fig. 8) comprising of a synchronous generator (SG), a PMSG-based WT, and a local load is built up on the simulation platform DIgSILENT/PowerFactory. The nominal capacity of SG is set as 4.9MVA; the rated power factor is 0.8; and the droop parameter of its governor is 4%. For the PMSG-based WT, its rated power is 1.5MW, and other parameters are referred to Appendix. A fixed load model is set as P_L+Q_L=3MW+0.2MVAR. In practice, the selection of N for the EMA algorithm is dependent on the practical requirements of the trade-off between power smoothing performance and total wind energy harvesting capability. In the case studies, N is equal to 80 per second as an example case to demonstrate the overall smoothing performance of different control strategies, and k is equal to 2/(80+1).

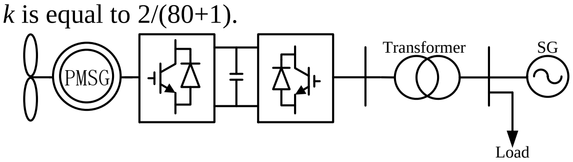

Fig. 8. Diagram of the test system

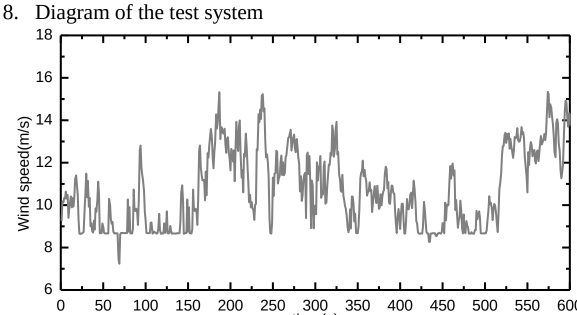

Fig. 9. Wind speed time series used in case study

B. Control Performance of Individual Strategy

The simulation result is shown in this subsection to test the effectiveness of individual control strategy using DC-link voltage, rotor speed, and pitch angle respectively. Fig. 9 gives the time-varying wind speed used in simulations. The power smoothing results with different control strategies as well as the behavior of the rotor speed, DC-link voltage and pitch angle are discussed as follows.

1) DC-link voltage control

The power smoothing effect of DC-link voltage control can be verified via comparing the WT output profiles of the proposed control and the conventional MPPT control. As shown in Fig. 10(a), the power fluctuation is slightly reduced through DC-link voltage control. However, the smoothing effect is non-significant due to the capacity limitation of DC-link capacitor. Once DC-link voltage reaches its upper/lower limit, DC-link capacitor cannot assist in power smoothing anymore and the output power is determined by the MPPT control again. Fig. 10(c) shows that the DC-link voltage varies within the acceptable range when the DC-link voltage control is implemented. Since DC-link voltage control does not affect the MPPT control, the rotor speed and pitch angle remain the same with the conventional MPPT control, as shown in Fig. 10(d, e).

2) Rotor Speed Control

The smoothed power output of PMSG-based WT using rotor speed control is shown in Fig. 10(a). The rotor speed variation is shown in Fig. 10(d). Visually, given the same smoothing command, the rotor speed control outperforms DC- link voltage control since WT rotational system contains larger power capacity. On the other hand, the rotor speed control causes significant speed variations as compared to the conventional MPPT control since additional acceleration or deceleration of the rotor is used to smooth power fluctuations. The control performance is relatively better when output power needs decrease compared with the situation when output power should increase. For example, during the period from 350s to 500s, the smoothing command is larger than MPPT point and the control command requests rotor to decelerate to release more power to match the smoothing command. In this situation, the energy released from the rotating rotor is marginal as compared with the energy loss caused by non-MPP operation state. Therefore, we set the lower bound of rotor speed

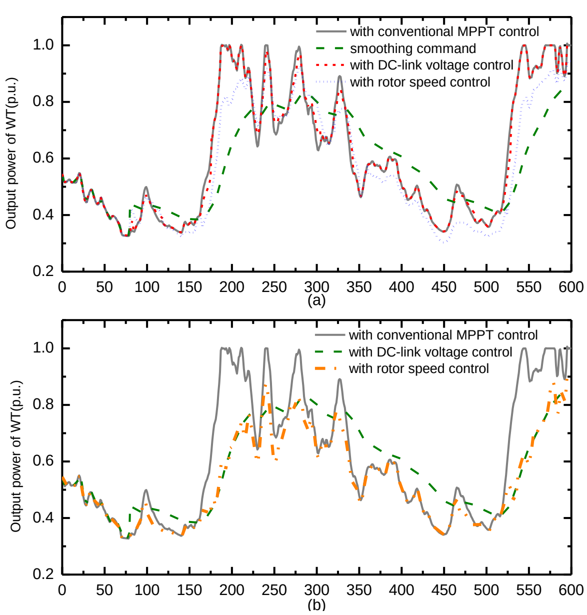

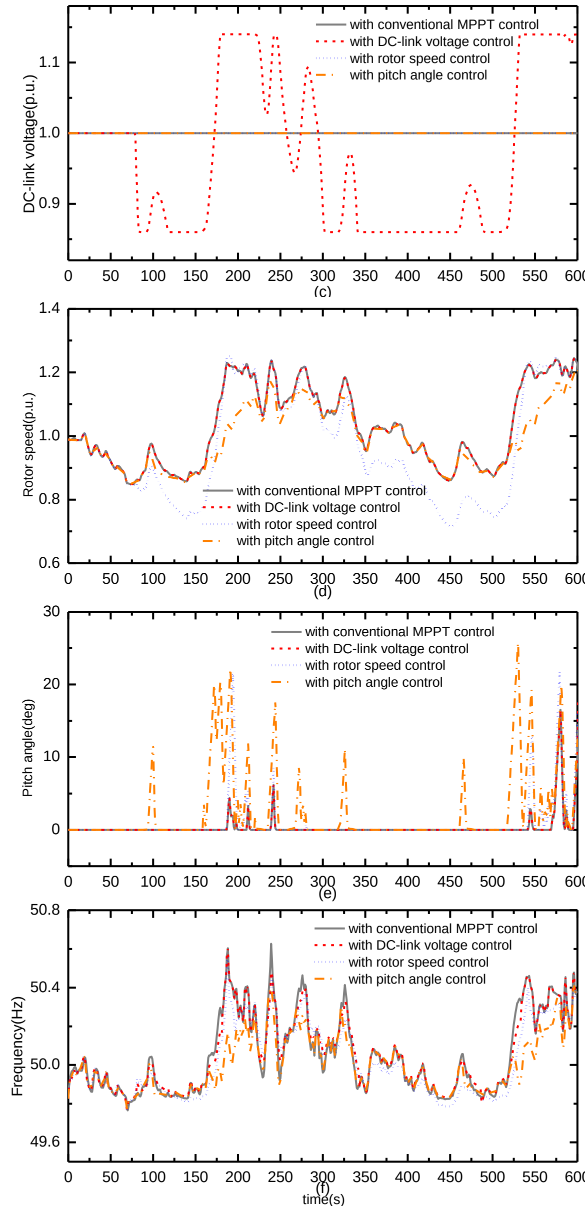

Fig. 10. Simulation results for individual control strategy (a). Output power of PMSG-based WT, (b). Output power of PMSG-based WT, (c). DC-link voltage, (d). Rotor speed, (e). Pitch angle, (f) System frequency

deceleration (i.e. ω_{opt}) when allocating smoothing task to the rotor speed control in this work.

3) Pitch Angle Control

The output power of PMSG-based WT using pitch angle control is presented in Fig. 10(b), where power fluctuation is effectively reduced. Fig. 10(e) indicates that the activation of pitch angle becomes more frequent as compared to other control strategies. It should be noted that the smoothing command cannot be tracked rapidly and precisely through pitch angle control. Occasionally, there exists instances that pitch angle control brings about counterproductive effect in power smoothing. For example, during the periods from 227s to 235s and from 250s to 264s, more power is supposed to be generated according to smoothing command, however, the pitch angle fails to retain zero as exhibited in Fig. 10(b). The reason is that pitch angle control is generally slow-responding due to its mechanical characteristics.

C. Combination of DC-link Voltage Control and Rotor Speed Control

Simulation results of case studies taking the combination of DC-link voltage control and rotor speed control into consideration are shown in Fig. 11. It can be seen from Fig. 11(b-c) that when *N*=80, the smoothing capabilities of DC-link capacitor and rotational rotor are both exploited adequately to follow the smoothing command no matter with simultaneous control and hierarchical control. To further demonstrate the advantage of hierarchical control on rationally utilizing existing resource to provide smoothing support and reducing energy loss, the scenario when *N*=10 is also considered. It can be seen from Fig. 12(b) that the DC-link capacitor always has a high priority to utilize when smoothing deviation is detected, and then more energy can be released back when more wind power is expected. By comparison, it can be found that when *N*=10, the smoothing deviation [1] is 0.0244 with the simultaneous control. In the case that hierarchical control is adopted, the smoothing deviation is reduced to 0.0133. The total captured wind energy is 147.364k·h via the simultaneous control and the captured wind energy increases to 150.024kW·h via the hierarchical control. In the case *N*=80, the smoothing deviation is 0.0941 and the captured wind energy is 139.239kW·h when the simultaneous control is implemented. While when hierarchical control is utilized, the smoothing deviation decreases to 0.0855 and the captured wind energy increases to 144.515 kW·h.

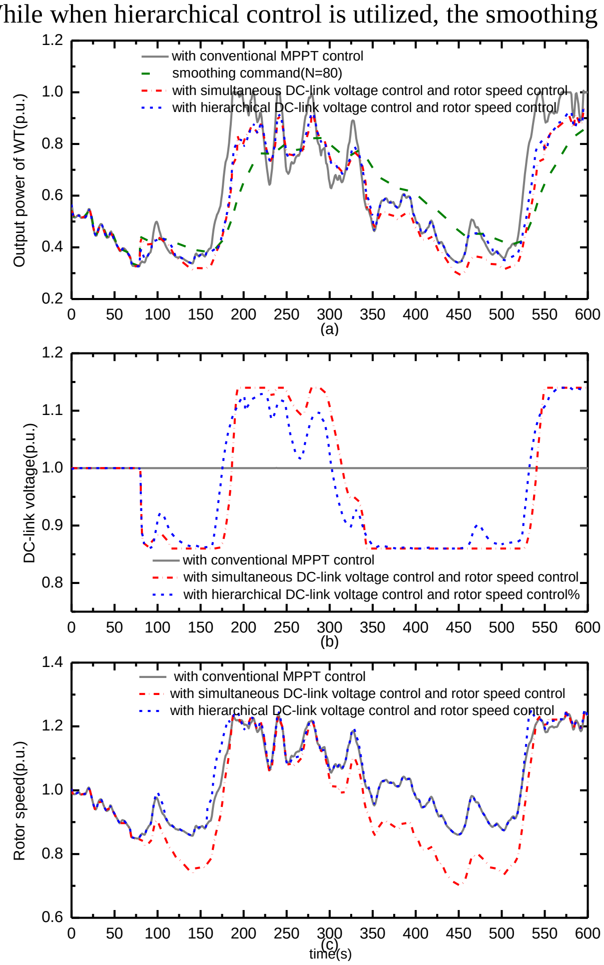

Fig. 11. Simulation results for combination of DC-link voltage control and rotor speed control(*N*=80) (a). Output power of PMSG-based WT, (b). DC-link voltage, (c). Rotor speed

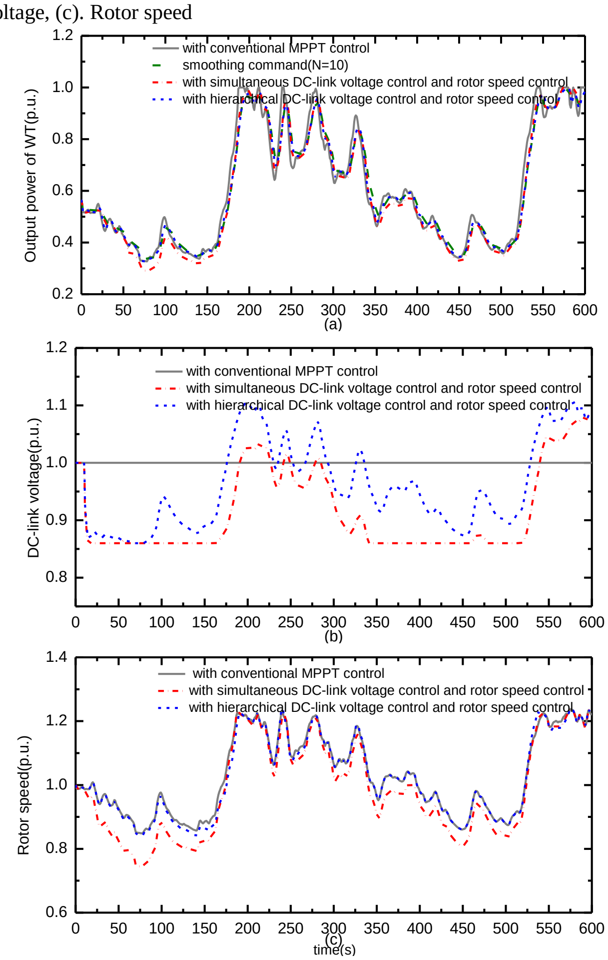

Fig. 12. Simulation results for combination of DC-link voltage control and rotor speed control(*N*=10) (a). Output power of PMSG-based WT, (b). DC-link voltage, (c). Rotor speed

D. Simultaneous Control Strategy

Simultaneous control integrates all controllers mentioned above whereas they concurrently tract the identical smoothing command and less coordinated. Fig. 13 shows the power smoothing results and exhibits that simultaneous control has better performance than individual control strategies and the smoothing command can be tracked rapidly in case active power should be reduced. In contrast, when more active power is demanded, the smoothing result is however less satisfactory. This is because the frequent actuation of pitch angle control inevitably leads to energy loss. Compared with individual control, activation frequency and the fluctuating magnitude of DC-link voltage, the rotor speed and the pitch angle are considerably reduced by deploying simultaneous control, which are shown in Fig. 13(b-d).

E. Hierarchical Control Strategy

The effectiveness of the proposed hierarchical control is demonstrated through Fig. 13. Via comparison, it is worth noting that the proposed hierarchical control outperforms simultaneous control especially when overloading is needed.

[1] Smoothing deviation is quantified to evaluate the smoothing performance of a specific control strategy, which is defined as: $\delta = \sqrt{1/N\sum_{i=1}^{N}(P_{meas} - P_{com})^2}$

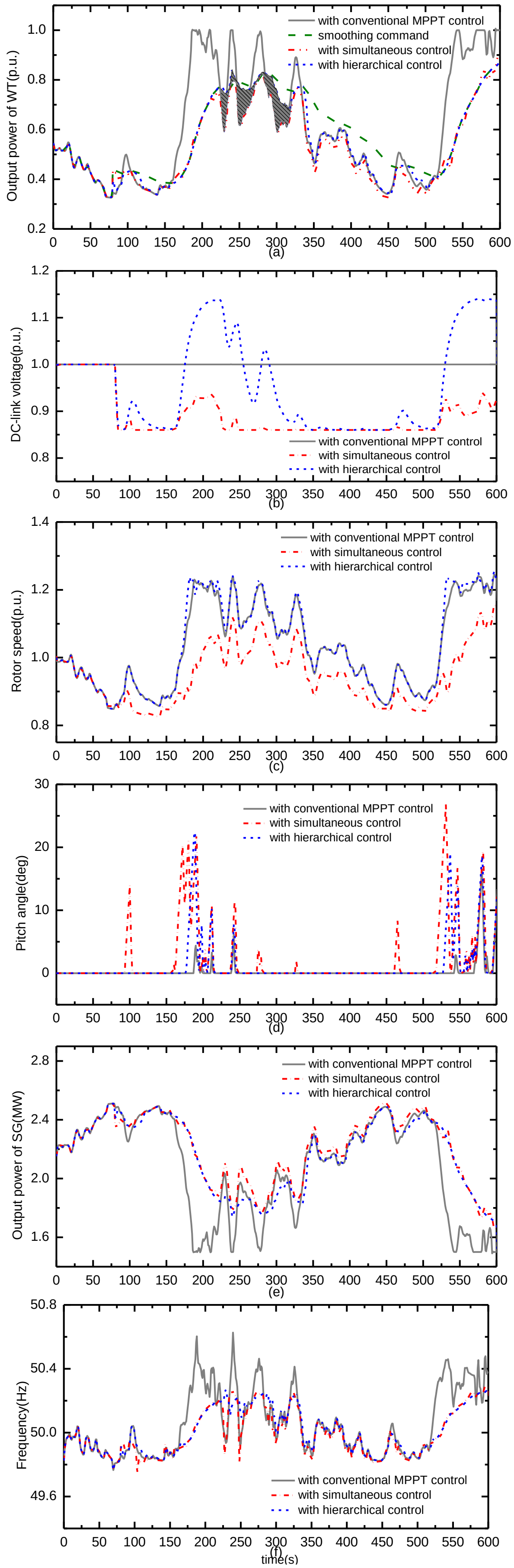

Fig. 13. Simulation results for simultaneous and hierarchical control (a). Output power of PMSG-based WT, (b). DC-link voltage, (c). Rotor speed, (d). Pitch angle, (e) Output power of SG, (f) System frequency

For example, as shown in the shadow areas marked in Fig. 13 (a), the difference of wind energy harvesting between the hierarchical control and simultaneous control is calculated to be 4.492kW·h. It can be hereby concluded that the proposed hierarchical control can supply more wind power support on overloading conditions. As the DC-link voltage and rotor speed are both adjusted in the acceptable range, this would lead to no additional cost in producing more power. Using the proposed hierarchical control strategy, the smoothing task is properly allocated to available resources and smoothing abilities of DC-link capacitor and rotational rotor are utilized to the greatest extent. As a result, the pitch angle control activates less frequently in hierarchical control, as shown in Fig. 13(d). Due to better performance of the hierarchical control, the frequency deviation is well mitigated as compared to simultaneous control and conventional MPPT control, as shown in Fig. 13(f). To make a quantitative comparison, the standard deviation of system frequency throughout 600s is calculated respectively with the sampling time of 1s. The standard deviation of frequency is 0.206 via conventional MPPT control. In the case that the simultaneous control is implemented, the frequency deviation decreases to 0.141. When the hierarchical control is utilized, the frequency deviation is reduced to 0.139. Consequently, the output power fluctuation of SG is significantly alleviated, which reduces the tear and wear and maintenance costs. From Figs 13, the deviation between the actual power output and the smoothing command through simultaneous control strategy and hierarchical control strategy, the actuation time of pitch angle and total captured wind energy are quantified and listed in Table I. It is obvious that the proposed hierarchical control outperforms the simultaneous control method in terms of 1) smaller smoothing deviation; 2) less WT mechanical fatigue; and 3) more harvested wind energy.

TABLE I Comparison of Different Control Strategies

	MPPT control	Simultaneous control	Hierarchical control
Smoothing deviation	0.1483	0.0721	0.0558
Actuation time of pitch angle	61s	187s	120s
Total captured wind energy	151.988 kW·h	132.306 kW·h	137.681 kW·h

VI. Conclusion

This paper comprehensively investigates two novel control strategies for wind power smoothing. The first one utilizes the DC-link voltage control, rotor speed control and pitch angle control simultaneously to tract the identical smoothing command. To pursue a better smoothing performance, the proposed hierarchical control seeks to coordinate these three controllers in an optimal manner. The simulation results exhibit that the proposed hierarchical control can effectively mitigate wind power fluctuations and harvest more energy as compared to simultaneous control. Further work is underway to investigate smoothing strategy from the perspective of wind farms by considering wind speed correction with respect to time and space.

VII. APPENDIX

TABLE A Parameters of PMSG-based Wind Turbine

Symbol	Item	Value
V_{rated}	Rated wind speed	14m/s
T_β	Time constant of the pitch serve	0.5 s
J_{tur}	Turbine inertia	6100000kgm^2
R	Rotor blade radius	30m
P_{rated}	Rated power	1.5 MW
U_g	Terminal Voltage	3.3 kV
J_{gen}	Generator inertia	130kgm^2
C	Capacitance of DC-link capacitor	0.075F
$U_{dcrated}$	Rated DC-link voltage	7.1kV
$\Delta P_c^{\max}$	Maximum active power support provided by DC-link capacitor	0.1p.u.
$\Delta P_R^{\max}$	Maximum active power support provided by rotational rotor	0.2p.u.

VIII. REFERENCES

[1] N. S. Naidu, and B. Singh, "Grid-interfaced DFIG-based variable speed wind energy conversion system with power smoothening," *IEEE transactions on sustainable energy,* vol. 8, no. 1, pp. 51-58, 2017.

[2] P. Sorensen, N. A. Cutululis, A. Vigueras-Rodríguez *et al.*, "Power fluctuations from large wind farms," *IEEE Transactions on Power Systems,* vol. 22, no. 3, pp. 958-965, 2007.

[3] Y. Jia, Y. Gao, Z. Xu *et al.*, "Powering China's sustainable development with renewable energies: current status and future trend," *Electric Power Components and Systems,* vol. 43, no. 8-10, pp. 1193-1204, 2015.

[4] A. M. Howlader, N. Urasaki, A. Yona *et al.*, "A review of output power smoothing methods for wind energy conversion systems," *Renewable and Sustainable Energy Reviews,* vol. 26, pp. 135-146, 2013.

[5] B. Ni, and C. Sourkounis, "Energy yield and power fluctuation of different control methods for wind energy converters." pp. 1-7.

[6] Y. Li, Z. Xu, and K. P. Wong, "Advanced control strategies of PMSG-based wind turbines for system inertia support," *IEEE Trans. Power Syst,* vol. 32, no. 4, pp. 3027-3037, 2017.

[7] G. Shafiullah, A. M. Oo, A. S. Ali *et al.*, "Potential challenges of integrating large-scale wind energy into the power grid–A review," *Renewable and sustainable energy reviews,* vol. 20, pp. 306-321, 2013.

[8] J. C. Smith, M. R. Milligan, E. A. DeMeo *et al.*, "Utility wind integration and operating impact state of the art," *IEEE transactions on power systems,* vol. 22, no. 3, pp. 900-908, 2007.

[9] G. Strbac, "Quantifying the system costs of additional renewables in 2020," *DTI report*, 2002.

[10] D. J. Swider, and C. Weber, "The costs of wind's intermittency in Germany: application of a stochastic electricity market model," *International Transactions on Electrical Energy Systems,* vol. 17, no. 2, pp. 151-172, 2007.

[11] T. Ackermann, *Wind power in power systems*: John Wiley & Sons, 2005.

[12] Q. Jiang, and H. Hong, "Wavelet-based capacity configuration and coordinated control of hybrid energy storage system for smoothing out wind power fluctuations," *IEEE Transactions on Power Systems,* vol. 28, no. 2, pp. 1363-1372, 2013.

[13] F. Diaz-Gonzalez, F. D. Bianchi, A. Sumper *et al.*, "Control of a flywheel energy storage system for power smoothing in wind power plants," *IEEE Transactions on Energy Conversion,* vol. 29, no. 1, pp. 204-214, 2014.

[14] W. Guo, L. Xiao, and S. Dai, "Enhancing low-voltage ride-through capability and smoothing output power of DFIG with a superconducting fault-current limiter–magnetic energy storage system," *IEEE Transactions on Energy Conversion,* vol. 27, no. 2, pp. 277-295, 2012.

[15] H. M. Hasanien, "A set-membership affine projection algorithm-based adaptive-controlled SMES units for wind farms output power smoothing," *IEEE Transactions on Sustainable Energy,* vol. 5, no. 4, pp. 1226-1233, 2014.

[16] G. Suvire, and P. Mercado, "Active power control of a flywheel energy storage system for wind energy applications," *IET Renewable Power Generation,* vol. 6, no. 1, pp. 9-16, 2012.

[17] F. Zhang, K. Meng, Z. Xu *et al.*, "Battery ESS planning for wind smoothing via variable-interval reference modulation and self-adaptive SOC control strategy," *IEEE Transactions on Sustainable Energy,* vol. 8, no. 2, pp. 695-707, 2017.

[18] M. Chowdhury, N. Hosseinzadeh, and W. Shen, "Smoothing wind power fluctuations by fuzzy logic pitch angle controller," *Renewable Energy,* vol. 38, no. 1, pp. 224-233, 2012.

[19] T. Senjyu, R. Sakamoto, N. Urasaki *et al.*, "Output power leveling of wind turbine generator for all operating regions by pitch angle control," *IEEE Transactions on Energy conversion,* vol. 21, no. 2, pp. 467-475, 2006.

[20] A. M. Howlader, N. Urasaki, T. Senjyu *et al.*, "Output power smoothing of wind turbine generation system for the 2-MW permanent magnet synchronous generators." pp. 452-457.

[21] Y. Kim, M. Kang, E. Muljadi *et al.*, "Power Smoothing of a Variable-Speed Wind Turbine Generator in Association With the Rotor-Speed-Dependent Gain," *IEEE Transactions on Sustainable Energy,* vol. 8, no. 3, pp. 990-999, 2017.

[22] S. G. Varzaneh, G. Gharehpetian, and M. Abedi, "Output power smoothing of variable speed wind farms using rotor-inertia," *Electric Power Systems Research,* vol. 116, pp. 208-217, 2014.

[23] A. M. Howlader, T. Senjyu, and A. Y. Saber, "An integrated power smoothing control for a grid-interactive wind farm considering wake effects," *IEEE Systems Journal,* vol. 9, no. 3, pp. 954-965, 2015.

[24] A. Uehara, A. Pratap, T. Goya *et al.*, "A coordinated control method to smooth wind power fluctuations of a PMSG-based WECS," *IEEE Transactions on energy conversion,* vol. 26, no. 2, pp. 550-558, 2011.

[25] A. D. Hansen, C. Jauch, P. Sørensen *et al.*, "Dynamic wind turbine models in power system simulation tool DIgSILENT," *Report Risoe*, pp. 1-80, 2003.

[26] M. F. M. Arani, and Y. A.-R. I. Mohamed, "Assessment and enhancement of a full-scale PMSG-based wind power generator performance under faults," *IEEE Transactions on Energy Conversion,* vol. 31, no. 2, pp. 728-739, 2016.

[27] Q. Jiang, and H. Wang, "Two-time-scale coordination control for a battery energy storage system to mitigate wind power fluctuations," *IEEE Transactions on Energy Conversion,* vol. 28, no. 1, pp. 52-61, 2013.

[28] X. Zhao, Z. Yan, and X.-P. Zhang, "A wind-wave farm system with self-energy storage and smoothed power output," *IEEE Access,* vol. 4, pp. 8634-8642, 2016.

[29] J. Zhao, X. Lyu, Y. Fu *et al.*, "Coordinated microgrid frequency regulation based on DFIG variable coefficient using virtual inertia and primary frequency control," *IEEE Transactions on Energy Conversion,* vol. 31, no. 3, pp. 833-845, 2016.

[30] J. Zhu, C. D. Booth, G. P. Adam *et al.*, "Inertia emulation control strategy for VSC-HVDC transmission systems," *IEEE Transactions on Power Systems,* vol. 28, no. 2, pp. 1277-1287, 2013.

Lyu Xue (S'16) received the B.Eng. degree from Qingdao University of Technology, China, in 2013. And the M. Eng. Degree from Shanghai University of Electric Power, China, in 2016, respectively. She is currently working toward the Ph.D. degree in the Department of Electrical Engineering, The Hong Kong Polytechnic University, Hong Kong. Her main research interest is renewable energy integration.

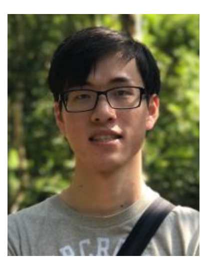

(S'15) received the B.Eng. degree from Zhejiang University, China, in 2013, and the Ph.D. degree from Hong Kong Polytechnic University, in 2017. He is currently with the Department of Electrical Power Engineering, Shanghai University of Electric Power, Shanghai, China. He was a research assistant at Hong Kong Polytechnic University and a visiting scholar at Argonne National Laboratory, Argonne, IL, USA. His research interests include distribution network operation and planning, grid integration of electric vehicles and renewable energies. Dr. Zhao was a recipient of the 2016 IEEE PES Best Paper Award.

Youwei Jia (S'11, M'15) received his B.Eng and Ph.D degrees from Sichuan University, China, in 2011, and The Hong Kong Polytechnic University, Hong Kong, in 2015, respectively. He is now with The Hong Kong Polytechnic University as a postdoctoral fellow. His research interests include microgrid, power system security analysis, cascading failures, complex network and artificial intelligence application in power engineering.

Zhao Xu (M'06-SM'12) received B.Eng, M.Eng and Ph.D degree from Zhejiang University, National University of Singapore, and The University of Queensland in 1996, 2002 and 2006, respectively. From 2006 to 2009, he was an Assistant and later Associate Professor with the Centre for Electric Technology, Technical University of Denmark, Lyngby, Denmark. Since 2010, he has been with The Hong Kong Polytechnic University, where he is currently a Professor in the Department of Electrical Engineering and Leader of Smart Grid Research Area (http://www.mypolyuweb.hk/eezhaoxu/). He is also a foreign Associate Staff of Centre for Electric Technology, Technical University of Denmark. His research interests include demand side, grid integration of wind and solar power, electricity market planning and management, and AI applications. He is an Editor of the Electric Power Components and Systems, the IEEE PES Power Engineering Letter, and the IEEE Transactions on Smart Grid. He is currently the Chairman of IEEE PES/IES/PELS/IAS Joint Chapter in Hong Kong Section.

Kit Po Wong (M'87–SM'90–F'02) received the M.Sc., Ph.D., and D.Eng. degrees from the Institute of Science and Technology, University of Manchester, Manchester, U.K., in 1972, 1974, and 2001, respectively. Since 1974, he has been with the School of Electrical, Electronic, and Computer Engineering, University of Western Australia, Australia, where he is currently a Winthrop Professor. His current research interests include power system analysis, planning and operations, and smart grids. Prof. Wong received three Sir John Madsen Medals (1981, 1982, and 1988) from the Institution of Engineers Australia, the 1999 Outstanding Engineer Award from the IEEE Power Chapter Western Australia, and the 2000 IEEE Third Millennium Award. He was the Editor-inChief of the IEE Proceedings in Generation, Transmission, and Distribution and the Editor-in-Chief of the IEEE POWER ENGINEERING LETTERS